Proceedings of IPACK2007
ASME InterPACK '07
July 8-12, 2007, Vancouver, British Columbia, CANADA

IPACK2007-33636

ANALYTICAL MODELING OF FLUID FLOW AND HEAT TRANSFER IN MICRO/NANO-CHANNEL HEAT SINKS

Waqar A. Khan
Associate Professor
Department of Mathematics
CIIT Abbottabad, NWFP, Pakistan
Email: wkhan@ciit.net.pk

Michael M. Yovanovich
Distinguished Professor Emeritus
Department of Mechanical Engineering
University of Waterloo, Waterloo, Canada, N2L 3G1
mmyov@uwaterloo.ca

ABSTRACT

Laminar forced convection in two-dimensional rectangular micro and nano-channels under hydrodynamically and thermally fully developed conditions is investigated analytically in the slip flow regime $(0.001 < Kn < 0.1)$*. Closed form solutions for fluid friction and Nusselt numbers are obtained by solving the continuum momentum and energy equations with the first-order velocity slip and temperature jump boundary conditions at the channel walls. Isoflux thermal boundary condition is applied on the heat sink base. Results of the present analysis are presented in terms of channel aspect ratio, hydraulic diameter, momentum and thermal accommodation coefficients, Knudsen number, slip velocity, Reynolds number and Prandtl number. It is found that fluid friction decreases and heat transfer increases, compared to no-slip flow conditions, depending on aspect ratios and Knudsen numbers that include effects of the channel size or rarefaction and the fluid/wall interaction.*

INTRODUCTION

Conventional heat sinks and heat pipes are unable to handle high heat removal rates. After the pioneering work of Tuckerman and Pease [1], microchannel heat sinks have received considerable attention especially in microelectronics. Most of these microchannel heat sinks were water-cooled. They could dissipate extremely high-power density with a heat flux as high as $790 W/cm^2$ [Tuckerman and Pease]. These heat sinks do not include slip effect.

In micro/nano-channels, the gas flow can be modeled using Navier-Stokes and energy equations using first-order slip flow and temperature jump boundary conditions . Microscopic effects become more important when the molecular mean free path of the coolant gas has the same order of magnitude as the channel size. Due to these effects, friction factors decrease and heat transfer coefficients increase with increase in Knudsen number.

In this study, the fully developed laminar flow is analyzed through rectangular micro/nano-channels in the slip flow regime $(0.001 < Kn < 0.1)$ and closed form solutions are obtained for friction factors and heat transfer coefficients in terms of channel aspect ratio, Knudsen number, Reynolds number and Prandtl number.

There is currently no model for predicting corresponding velocity profiles or pressure distribution in the slip regime. Moreover, there is no such model that can be used in other geometries, e.g., two-dimensional channels and rectangular ducts with different aspect ratios. The objective of the current investigation is to develop a unified, physics-based model appropriate for slip-flow regime and for two-dimensional channels, and ducts.

Literature Review

In the last two decades, the flow and heat transfer in micro/nano-channel heat sinks have become a subject of growing research attention in microelectronics. Although the work on these channels is not new, but after Tuckerman and Pease [1], microchannel heat sinks have received considerable attention especially in microelectronics. Following this work, several experimental, numerical and theoretical studies on rarefied gas flows in microchannels have been carried out in a wide range of Knudsen

number with the objective of developing simple, physics-based models. These studies are reviewed in this section.

Harley et al. [2] and then later on Morini and his coworkers [3-5] presented analytical and experimental studies. In these studies, they investigated the rarefaction effects on the pressure drop through silicon microchannels having rectangular, trapezoidal or double-trapezoidal cross-section. They pointed out the roles of the Knudsen number and the cross-section aspect ratio in the friction factor reduction due to the rarefaction and obtained solutions for velocity profiles, friction factors, shear stresses, momentum flux, and kinetic energy correction factors.

Ebert and Sparrow [6] formulated an analytical slip-flow solution for a rectangular channel. They found that the effect of slip is to flatten the velocity distribution relative to that for a continuum flow and the compressibility increases the pressure drop through an increase in viscous shear rather than through an increase in momentum flux.

Inman [7-9] presented theoretical analyzes for the fluid flow and heat transfer for laminar slip flow in a parallel plate channel with different thermal boundary conditions. The solutions contain a series expansion, and analytical expressions for the complete set of eigenvalues and eigenfunctions for the problems. They obtained expressions for the temperature of the gas adjacent to the wall , the wall heat flux, and the Nusselt numbers for the conduits for various values of the rarefaction parameters. The results indicate that the thermal entrance length is decreased with increasing gas rarefaction and also that for a given mean free path the thermal entrance length is greater for unsymmetrical heating than for a symmetrical wall heat flux.

Colin et al. [10] proposed an analytical slip-flow model based on second-order boundary conditions for gaseous flow in rectangular microchannels. They designed an experimental setup for the measurement of gaseous micro flow rates under controlled temperature and pressure conditions. It was shown that in rectangular microchannels, the proposed second-order model is valid for Knudsen numbers up to about 0.25, whereas the first-order model is no longer accurate for values higher than 0.05. The best fit is found for a tangential momentum accommodation coefficient $\sigma = 0.93$, both with helium and nitrogen. Yu and Ameel [11, 12] investigated analytically the laminar forced convection in thermally developing slip flow through isoflux rectangular microchannels. They obtained local and fully developed Nusselt numbers, fluid temperatures, and wall temperatures by solving the continuum energy equation for hydrodynamically fully developed slip flow with the velocity slip and temperature jump condition at the walls. They found that heat transfer may increase, decrease, or remain unchanged, compared to nonslip flow conditions, depending on aspect ratios and two-dimensionless variables that include effects of the microchannel size or rarefaction and the fluid/wall interaction.

Zhao and Lu [13] presented an analytical and numerical study on the heat transfer characteristics of forced convection across a microchannel heat sink. They used porous medium and fin approaches and investigated the effects of channel aspect ratio and effective thermal conductivity ratio on the overall Nusselt number. They found that the overall Nusselt number increases as channel aspect ratio is increased and decreases with increasing effective thermal conductivity ratio. They proposed a new concept of microchannel cooling in combination with microheat pipes and estimated the enhancement in heat transfer. They conducted two-dimensional numerical calculations for both constant heat flux and constant wall temperature conditions to check the accuracy of the analytical solutions and to examine the effect of different boundary conditions on the overall heat transfer.

Quarmby [14] and Gampert [15] used finite-difference simulations to investigate developing slip flow in circular pipes and parallel plates.

Barber and Emerson [16, 17] examined the role of Reynolds and Knudsen numbers on the hydrodynamic development length at the entrance to parallel plate microchannels. They carried out numerical simulations over a range of Knudsen numbers covering the continuum and slip-flow regimes. Their results demonstrate that at the upper limit of the slip-flow regime, the entrance development region is almost 25% longer than that predicted using continuum flow theory.

Andrei and Raymond [18] developed a three-dimensional model to investigate flow and conjugate heat transfer in the microchannel-based heat sink for electronic packaging applications. They solved the Navier-Stokes equations of motion numerically using the generalized single equation framework. They also developed and validated the theoretical model by comparing the predictions of the thermal resistance and the friction coefficient with available experimental data for a wide range of Reynolds numbers. Their analysis provides a unique fundamental insight into the complex heat flow pattern established in the channel due to combined convection-conduction effects in the three-dimensional setting.

Arkilic et al. [19, 20] performed analytic and experimental investigations into gaseous flow with slight rarefaction through long microchannels. They used a two-dimensional (2-D) analysis of the Navier-Stokes equations with a first-order slip-velocity boundary condition to demonstrate that both compressibility and rarefied effects are present in long microchannels. They reported the tangential momentum accommodation coefficients (TMAC) for nitrogen, argon and carbon dioxide gases in contact with single-crystal silicon. For all three gases the TMAC is found to be lower than one, ranging from 0.75 to 0.85.

Beskok and Karniadakis [21] developed simple, physics-based models for flows in channels, pipes and ducts at micro scales for a wide range of Knudsen number at low Mach number. They proposed a new general boundary condition that accounts for the reduced momentum and heat exchange with wall surfaces and investigated its validity. They found that as the value of Knudsen number increases, rarefaction effects become more

important and thus pressure drop, shear stress, heat flux, and corresponding mass flow rate cannot be predicted from standard flow and heat transfer models based on the continuum hypothesis. They also explored that simple models based on kinetic gas theory concepts are not appropriate either, except in the very high Knudsen number regime corresponding to near-vacuum conditions.

Bower et al. [22] presented experimental results on the heat transfer and flow in small SiC heat exchangers with multiple rows of parallel channels oriented in the flow direction. They analyzed overall heat transfer and pressure drop coefficients in single phase flow regimes and found that liquid-cooled SiC heat sinks easily outperform air-cooled heat sinks.

Harms et al. [23] obtained experimental results for single-phase forced convection in deep rectangular microchannels. They tested single and multiple channel systems. All tests were performed with deionized water as the working fluid, where the Reynolds number ranged from 173 to 12,900. The experimentally obtained local Nusselt number agrees reasonably well with classical developing channel flow theory. Furthermore, their results show that multiple channel system designed for developing laminar flow outperforms the comparable single channel system designed for turbulent flow.

Hetsroni et al. [24, 25] performed experimental and theoretical investigations on single-phase fluid flow and heat transfer in micro-channels. They considered both problems in the frame of a continuum model, corresponding to small Knudsen number. They analyzed the data of pressure drop and heat transfer in circular, triangular, rectangular, and trapezoidal micro-channels. The effects of geometry, axial heat flux due to thermal conduction through the working fluid and channel walls, as well as the energy dissipation are discussed. They compared experimental data, obtained by a number of investigators, to conventional theory on heat transfer.

Hsieh et al. [26, 27] presented experimental and theoretical studies of incompressible and compressible flows in a microchannel. They used nitrogen and deionized water as working media in their experiments. The results were found in good agreement with those predicted by analytical solutions in which a 2-D continuous flow model with first slip boundary conditions are employed and solved by a perturbation method with a proposed new complete momentum accommodation coefficient.

NOMENCLATURE

A	total heating surface area, m^2
A_c	cross-section area of a single fin, m^2
D_h	hydraulic diameter, m
f	friction factor
G	volume flow rate, cm^3/s
H_c	channel height, m
h	average heat transfer coefficient, $W/m^2 \cdot K$
Kn	Knudsen number $\equiv \lambda/D_h$
k	thermal conductivity of solid, $W/m \cdot K$
k_f	thermal conductivity of fluid, $W/m \cdot K$
L	length of channel in flow direction, m
m	fin parameter, m^{-1}
$\dot{m}$	total mass flow rate, kg/s
N	total number of micro/nano-channels
Nu_{D_h}	Nusselt number based on hydraulic diameter
Pe_{D_h}	Peclet number based on hydraulic diameter
Pr	Prandtl number
Q_b	heat transfer rate from heat sink base, W
Q_{fin}	heat transfer rate from fin, W
q	heat flux, W/m^2
Re_{D_h}	Reynolds number based on hydraulic diameter
T	absolute temperature, K
t	thickness, m]
U_{av}	average velocity in channels, m/s
W	width of heat sink, m
w_c	half of the channel width, m
w_w	half of the fin thickness, m

Greek Symbols

ΔP	pressure drop across micro/nano-channel, Pa
α	thermal diffusivity, m^2/s or constant defined by Eq. (25)
α_c	channel aspect ratio $\equiv 2w_c/H_c$
α_{hs}	heat sink aspect ratio $\equiv L/2w_c$
β	fin spacing ratio $\equiv w_c/w_w$
γ	ratio of specific heats $\equiv c_p/c_v$
$\mathcal{L}$	characteristic length, m
λ	mean free path, m
μ	absolute viscosity of fluid, $kg/m \cdot s$
ν	kinematic viscosity of fluid, m^2/s
ρ	fluid density, kg/m^3
σ	tangential momentum accommodation coefficient
σ_t	energy accommodation coefficient
ζ_u	slip velocity coefficient
ζ_t	temperature jump coefficient

Subscripts

a	ambient
av	average
b	base surface
f	fluid
fin	single fin
g	gas
hs	heat sink
s	slip
th	thermal
w	wall

Assumptions

1. Uniform heat flux on the bottom surface.
2. Smooth surfaces of the channel
3. Adiabatic fin tips
4. Isotropic material
5. Steady, laminar, and fully developed heat and fluid flow
6. Slip flow (i.e., $0.001 \leq Kn \leq 0.1$) with negligible creep effects
7. Incompressible fluid with constant thermophysical properties
8. Negligible axial conduction in both the fin and fluid

Governing Equations

Continuum equations for conservation of mass, momentum and energy can be used with slip flow and temperature jump boundary conditions. Using scale analysis, the axial momentum and energy equations, for the control volume shown in Fig. 1 (b), reduces to:

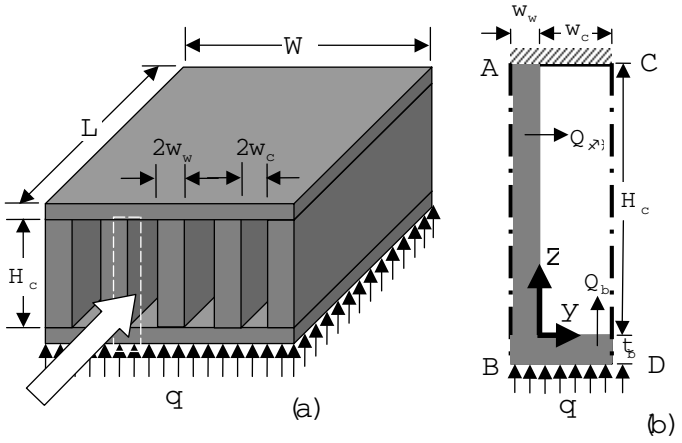

Fig. 1 MICRO/NANO-CHANNEL HEAT SINK: GEOMETRY, CONTROL VOLUME AND DEFINITIONS.

$$\frac{d^2u}{dy^2} = \frac{1}{\mu}\frac{dp}{dx} \tag{1}$$

and

$$u\frac{dT}{dx} = \alpha\frac{d^2T}{dy^2} \tag{2}$$

where dp/dx must be a (negative) constant to make u a positive quantity.

Hydrodynamic Boundary Conditions

(i) At the channel surface, i.e., at $y = 0$, the first-order slip boundary condition can be used

$$u = u_s = \xi_u \mathcal{L}\left.\frac{du}{dy}\right|_{y=0} \tag{3}$$

where $\mathcal{L}$ is the characteristic length, usually taken as the hydraulic diameter of the channel, D_h, and ξ_u is the slip velocity coefficient, given by

$$\xi_u = \left(\frac{2-\sigma}{\sigma}\right) Kn \tag{4}$$

where σ is the tangential momentum accommodation coefficient, given for different fluids and surfaces in Table 11-3 in Eckert and Drake [28], and Kn is the Knudsen number which lies between 0.001 and 0.1 in the slip flow region.

(ii) At the symmetry plane

$$y = w_c \qquad\qquad du/dy = 0 \tag{5}$$

Thermal Boundary Conditions

(i) Following Liu and Garimella [29], the thermal boundary condition at the base of the fin can be determined from an energy balance:

$$Q = Q_{fin} + Q_b \tag{6}$$

which gives

$$Q_{fin} = Q\left[\frac{Q_{fin}/Q_b}{1+(Q_{fin}/Q_b)}\right] \tag{7}$$

where

$$Q = q(w_w + w_c)L \tag{8}$$

$$Q_{fin} = h_{av}(H_c L)\eta_{fin}(T_b - T_f) \tag{9}$$

$$Q_b = h_{av}(w_c L)(T_b - T_f) \tag{10}$$

The efficiency of the fin η_{fin} in Eq. (9) with constant convective heat transfer coefficient and an insulated tip is:

$$\eta_{fin} = \frac{\tanh(mH_c)}{mH_c} \tag{11}$$

with the fin parameter $m = \sqrt{\frac{h_{av}}{k(2w_w)}}$.

Using these equations, Eq. (7) can be written as

$$Q_{fin} = q(w_w + w_c)L\left[\frac{2\eta_{fin}}{2\eta_{fin}+\alpha_c}\right] \tag{12}$$

Also

$$Q_{fin} = -k(w_w L)\left.\frac{\partial T}{\partial y}\right|_{y=0} \tag{13}$$

Combining Eqs. (12) and (13), we get

$$-k\left.\frac{\partial T}{\partial y}\right|_{y=0} = q\left(\frac{w_w + w_c}{w_w}\right)\left(\frac{2\eta_{fin}}{2\eta_{fin}+\alpha_c}\right) = q_w \tag{14}$$

where q_w is the flux on the channel wall.

(ii) The temperature jump at the wall can be written as

$$T_g - T_w = -\xi_t \mathcal{L}\left.\frac{dT}{dy}\right|_{y=0} \tag{15}$$

where ξ_t is the temperature jump coefficient and is defined as

$$\xi_t = \frac{2-\sigma_t}{\sigma_t}\cdot\frac{2\gamma}{\gamma+1}\cdot\frac{Kn}{Pr} \tag{16}$$

where σ_t is the thermal accommodation coefficient, γ is the ratio of specific heats and Pr is the Prandtl number.

(iii) At the symmetry plane

$$y = w_c \qquad dT/dy = 0 \tag{17}$$

(iv) At the top of the fin

$$z = H_c \qquad dT/dz = 0 \tag{18}$$

ANALYSIS

Fluid Flow

The pressure gradient term dp/dx in Eq. (1) can be written as

$$\frac{dp}{dx} = -\frac{\Delta P}{L} \tag{19}$$

So, Eq. (1) becomes

$$\frac{d^2u}{dy^2} = -\frac{1}{L\mu}\frac{\Delta P}{L} = 2A \tag{20}$$

where A is a constant and can be written as

$$A = -\frac{1}{2\mu}\frac{\Delta P}{L} \tag{21}$$

Integrating Eq. (20) twice w.r.t. y and using boundary conditions (Eqs. 3 and 5), we get

$$u(y) = -Aw_c^2[2(y/w_c) - (y/w_c)^2 + 4\alpha] \tag{22}$$

In terms of dimensionless variable η, velocity distribution can be written as

$$u(\eta) = -Aw_c^2(2\eta - \eta^2 + 4\alpha) \tag{23}$$

where

$$\eta = y/w_c \tag{24}$$

$$\alpha = 2\xi_u/(1+\alpha_c) \tag{25}$$

with the channel aspect ratio defined by

$$\alpha_c = \frac{2w_c}{H_c} \tag{26}$$

The average velocity in the channel is defined as

$$\begin{aligned} U_{av} &= \frac{1}{w_c}\int_0^{w_c} u(y)dy \\ &= -\frac{2}{3}Aw_c(1+6\alpha) \end{aligned} \tag{27}$$

The normalized velocity distribution and slip flow velocity can be written as

$$\left.\begin{aligned} \frac{u(\eta)}{U_{av}} &= \frac{3}{2}\left(\frac{2\eta-\eta^2+4\alpha}{1+6\alpha}\right) \\ \frac{U_s}{U_{av}} &= \frac{6\alpha}{1+6\alpha} \end{aligned}\right\} \tag{28}$$

Shear stress at the channel wall is defined as

$$\tau_w = \mu \left.\frac{du}{dy}\right|_{y=0} = \frac{3}{4} \cdot \frac{\mu^2(1+\alpha_c)}{\rho w_c^2} \cdot \frac{Re_{D_h}}{1+6\alpha} \tag{29}$$

where Re_{D_h} is the Reynolds number based on hydraulic diameter and is given by

$$Re_{D_h} = \frac{U_{av} D_h}{\nu} \tag{30}$$

Momentum transfer to the channel wall can be expressed in terms of skin friction coefficient or friction factor, defined as

$$f = \frac{\tau_w}{\frac{1}{2}\rho U_{av}^2} = \frac{24}{Re_{D_h}} \cdot \frac{1}{1+\alpha_c} \cdot \frac{1}{1+6\alpha} \tag{31}$$

which gives the Poiseuille number fRe_{D_h} for rectangular micro/nano-channels in terms of aspect ratio α_c and slip velocity coefficient.

$$fRe_{D_h} = \frac{24}{1+\alpha_c} \cdot \frac{1}{1+6\alpha} \tag{32}$$

The values of the Poiseuille number are compared with analytical values quoted by Shah and London [30] and numerical values given by Morini et al. [4] in Table 1 for continuum flow (Kn = 0). Morini et al. [4] defined the reduction of the friction factor due to the rarefaction effect as follows:

$$\phi = \frac{(fRe_{Dh})|_{Kn}}{(fRe_{Dh})|_{Kn=0}} = \frac{1}{1+\frac{12}{1+\alpha_c}\left(\frac{2-\sigma}{\sigma}\right)Kn} \tag{33}$$

For a fixed cross-section, the friction factor reduction ϕ has been calculated by comparing the Poiseuille number for an assigned value of the Knudsen number with the value that the Poiseuille number assumes for Kn = 0 (i.e., continuum flow). The friction factor reduction ϕ depends on the channel aspect ratio and on the Knudsen number.

Table 2 shows the comparison of the present values of the friction factor reduction ϕ with the numerical values presented by Morini et al. [4] for some values of the Knudsen number between 0.001 and 0.1. It shows that ϕ decreases as Kn goes from 0.001 to 0.1; this result confirms that gas rarefaction reduces the friction between the gas and the micro/nano-channel walls. The reduction of the friction factor is stronger for rectangular micro/nano-channels with a small channel aspect ratio. For Kn = 0.1 the friction factor reduction ϕ reaches the minimum value 45.5, the value of ϕ becomes 56.5% for a square micro/nano-channel ($\alpha_c = 1$).

Table 1. **COMPARISON OF POISEUILLE NUMBERS fRe_{D_h} FOR MICRO/NANO-CHANNELS**

α_c	Poiseuille number fRe_{D_h}		
	Shah and London [30]	Morini et al. [4]	Present
0	24	24	24
0.2	19.07	19.07	20.00
0.4	16.37	16.37	17.14
0.6	14.98	14.98	15.00
0.8	14.37	14.37	13.33
1.0	14.22	14.22	12.00

The rectangular micro/nano-channels with a smaller channel aspect ratio have a higher value of α_c; hence for these micro/nano-channels the decrease of the friction factor with the Knudsen number is larger. In other words, the rarefaction effects appear to be higher in micro/nano-channels with smaller aspect ratios. This is due to the definition of the Knudsen number based on the hydraulic diameter of the channel.

It shows that the present values are in good agreement for rectangular micro/nano-channels with the previous results. This can be considered a good validation of the assumptions made in the present work.

The coefficient of pressure loss can be determined from

$$K = \frac{\Delta P}{\frac{1}{2}\rho U_{av}^2} = k_{ce} + f(L/D_h) \tag{34}$$

where k_{ce} is the sum of contraction and expansion losses in the channel. Kleiner et al. [31] used experimental data from Kays and London [32] and derived the following empirical correlation for the entrance and exit losses k_{ce} in terms of channel width and fin thickness:

$$k_{ce} = 1.79 - 2.32\left(\frac{w_c}{w_c+w_w}\right) + 0.53\left(\frac{w_c}{w_c+w_w}\right)^2 \tag{35}$$

Table 2. **COMPARISON OF FRICTION FACTOR REDUCTION (ϕ) FOR MICRO/NANO-CHANNELS**

α_c	Friction Factor Reduction (ϕ)			
	$Kn = 0.001$		$Kn = 0.01$	
	Morini et al. [4]	Present	Morini et al. [4]	Present
0.0	0.988	0.992	0.893	0.892
0.1	0.989	0.991	0.901	0.899
0.2	0.990	0.990	0.907	0.910
0.3	0.990	0.989	0.912	0.919
0.4	0.991	0.988	0.917	0.918
0.5	0.991	0.988	0.920	0.925
0.6	0.992	0.987	0.923	0.927
0.7	0.992	0.993	0.924	0.936
0.8	0.992	0.992	0.925	0.932
0.9	0.992	0.992	0.925	0.944
1.0	0.992	0.992	0.926	0.942

Heat Transfer

The energy equation (Eq. 2), in dimensionless form, can be written as

$$(1+2\alpha_c) f(\eta) \frac{\partial \Theta}{\partial \xi} = \frac{4}{Pe_{D_h}} \frac{\partial^2 \Theta}{\partial \eta^2} \tag{36}$$

where

$$\xi = \frac{x}{w_c} \qquad \eta = \frac{y}{w_c}$$

$$f(\eta) = \frac{3}{2}\left(\frac{2\eta - \eta^2 + 4\alpha}{1+6\alpha}\right) \qquad \Theta = \frac{T - T_a}{D_h q_w / k_f}$$

$$U_{av} = \frac{u}{f(\eta)} \qquad Pe_{D_h} = Re_{D_h} Pr$$

From an energy balance on a fluid element in the channel

$$\frac{dT}{dx} = \frac{\alpha (q_w / k_f)}{w_c U_{av}} \tag{37}$$

In dimensionless form, it can be written as

$$\frac{\partial \Theta}{\partial \xi} = \frac{1}{Pe_{D_h}} \tag{38}$$

Combining Eqs. (36) and (38), we get

$$\frac{\partial^2 \Theta}{\partial \eta^2} = \frac{1+\alpha_c}{4} f(\eta) = \left(\frac{1+\alpha_c}{4}\right)\left[\left(3\eta - \frac{3}{2}\eta^2\right) + \left(1 - 3\eta + \frac{3}{2}\eta^2\right)\frac{U_s}{U_{av}}\right] \tag{39}$$

In dimensionless form, Eq. (14) can be written as

$$-k \left.\frac{\partial \Theta}{\partial \eta}\right|_{\eta=0} = \frac{k_f w_c}{D_h} \tag{40}$$

Also, from continuity of temperature and heat flux at the solid-fluid interface,

$$-k \left.\frac{\partial \Theta}{\partial \eta}\right|_{\eta=0} = -k_f \left.\frac{\partial \Theta}{\partial \eta}\right|_{\eta=0} \tag{41}$$

Combining Eqs. (40) and (41), we get

$$\left.\frac{\partial \Theta}{\partial \eta}\right|_{\eta=0} = -\frac{w_c}{D_h} \tag{42}$$

Using this boundary condition and integrating Eq. (39) w.r.t. η, we get

$$\frac{\partial \Theta}{\partial \eta} = \left(\frac{1+\alpha_c}{4}\right)\left[\left(\frac{3}{2}\eta^2 - \frac{1}{2}\eta^3 - 1\right) + \left(\eta - \frac{3}{2}\eta^2 - \frac{1}{2}\eta^3\right)\frac{U_s}{U_{av}}\right] \tag{43}$$

From an overall energy balance on the fluid element, we get the following additional condition

$$\int_0^1 f(\eta) \cdot \Theta(\eta) d\eta = 0 \tag{44}$$

Integrating Eq. (43) and applying Eq. (44), we get

$$\Theta(\eta) = (1+\alpha_c)\left[\left(\frac{1}{8}\eta^3 - \frac{1}{32}\eta^4 - \frac{1}{4}\eta + \frac{17}{140}\right) + \frac{1}{210}\left(\frac{U_s}{U_{av}}\right)^2 + \left(\frac{1}{8}\eta^2 - \frac{1}{8}\eta^3 - \frac{1}{32}\eta^4 - \frac{3}{70}\right)\frac{U_s}{U_{av}}\right] \tag{45}$$

Integrating Eq. (38) and applying the condition $\Theta = \dfrac{T_g - T_a}{D_h q_w / k_f}$ at $\eta = 0$, we get

$$\frac{T_g - T_a}{D_h q_w / k_f} = \frac{\xi}{Pe_{D_h}} + \Theta(0) \tag{46}$$

where $\Theta(0)$ can be determined from Eq. (45). From Eq. (15), we get

$$\frac{T_g - T_w}{D_h q_w / k_f} = \xi_t \tag{47}$$

Combining Eqs. (46) and (47), we get

$$\frac{T_w - T_a}{D_h q_w / k_f} = \frac{\xi}{Pe_{D_h}} + \Theta(0) + \xi_t \tag{48}$$

By definition, the bulk temperature is given by

$$T_b = T_a + \frac{(D_h q_w / k_f)\xi}{Pe_{D_h}} \tag{49}$$

which gives

$$\frac{T_b - T_a}{D_h q_w / k_f} = \frac{\xi}{Pe_{D_h}} \tag{50}$$

Combining Eqs. (48) and (50), we get

$$\begin{aligned} \frac{T_w - T_b}{D_h q_w / k_f} &= \Theta(0) + \xi_t \\ &= (1+\alpha_c)\left[\frac{17}{140} - \frac{3}{70}\frac{U_s}{U_{av}} + \frac{1}{210}\left(\frac{U_s}{U_{av}}\right)^2\right] + \xi_t \end{aligned} \tag{51}$$

For UWF, the average heat transfer coefficient for the fin is defined as

$$h_{fin} = \frac{q_w}{T_w - T_b} \tag{52}$$

In dimensionless form it can be written as

$$Nu_{D_h} = \frac{h_{fin} D_h}{k_f}$$

$$\begin{aligned} &= \frac{1}{(1+\alpha_c)\left[\frac{17}{140} - \frac{3}{70}\frac{U_s}{U_{av}} + \frac{1}{210}\left(\frac{U_s}{U_{av}}\right)^2\right] + \xi_t} \\ &= \frac{140/17}{(1+\alpha_c)\left[1 - \frac{6}{17}\frac{U_s}{U_{av}} + \frac{2}{51}\left(\frac{U_s}{U_{av}}\right)^2\right] + \frac{140}{17}\xi_t} \end{aligned} \tag{53}$$

Overall Heat Transfer Coefficient For Heat Sink

Heat balance for the whole CV can be written as

$$Q = NQ_{fin} + Q_b \tag{54}$$

where

$$\left.\begin{aligned} Q &= (h\eta A)_{hs}\theta_b \\ Q_{fin} &= (hA\eta)_{fin}\theta_b \\ Q_b &= (hA)_b\theta_b \end{aligned}\right\} \tag{55}$$

which gives the overall average heat transfer coefficient for a micro/nano-channel heat sink:

$$h_{hs} = \frac{(N+1)(Ah\eta)_{fin} + (hA)_b}{(\eta A)_{hs}} \tag{56}$$

with

$$\left.\begin{aligned} N &= \frac{W - 2w_w}{2(w_c + w_w)} \\ A_{hs} &= NA_{fin} + A_b \\ \eta_{hs} &= 1 - \frac{NA_{fin}}{A_{hs}}(1 - \eta_{fin}) \\ A_{fin} &= 2H_c(2w_w + L) \\ A_b &= LW - (N+1)(2w_w L) \end{aligned}\right\} \tag{57}$$

The average heat transfer coefficient for the fin can be determined from Eq. (54) whereas h_b for the UWF boundary condition was determined by Khan et al. [33] and could be written as

$$h_b = 0.912\frac{k_f}{L}Re_L^{1/2}Pr^{1/3} \tag{58}$$

where Re_L is the Reynolds number based on the length of the baseplate and is defined as

$$Re_L = \frac{U_{av}L}{\nu} \tag{59}$$

CASE STUDIES AND DISCUSSION

The slip flow range ($0.001 < Kn < 0.1$) dictates the channel width for the flow of any gas through micro/nano-channels. For air ($\lambda = 69.2nm$), Fig. 2 shows that the channel width ranges from 35 μm to 350 nm. Qin and Li [34] have shown a novel technique in creating micro/nano-channels using a Nd:YAG laser in a dry process.

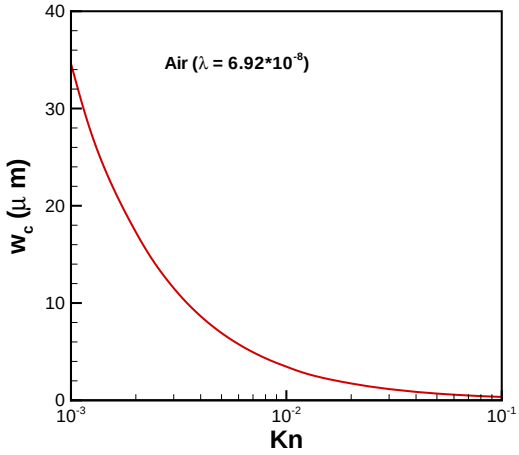

Fig. 2 CHANNEL WIDTH IN SLIP FLOW RANGE

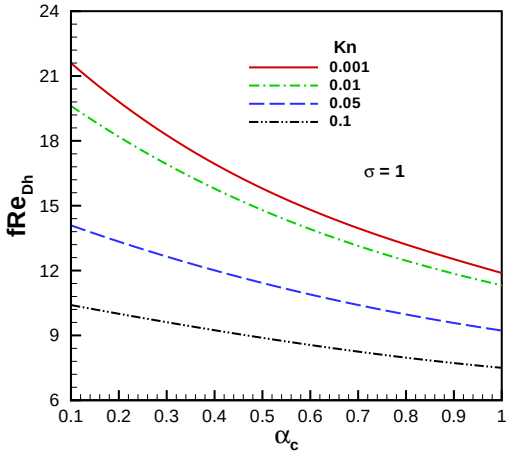

Fig. 3 EFFECT OF CHANNEL ASPECT RATIOS ON FRICTION FACTORS IN SLIP FLOW REGION

In these channels, friction losses are reduced as shown in Fig. 3. It is demonstrated that the friction losses are highest in the continuum flow ($Kn = 0$). As the Kn number increases, friction losses decrease with increase in aspect ratio. Arkilic et al. [19, 20] demonstrated experimentally that for nitrogen, argon and carbon dioxide, the TMAC is found to be lower than one, ranging from 0.75 to 0.85. The effect of these tangential momentum accommodation coefficients (TMAC) on the friction factors are shown in Fig. 4 in the slip region. It shows that the friction factors decrease monotonically as TMAC decreases and the channel aspect ratios increases. The effects of aspect ratios on the pressure drop in the slip flow region are investigated in Fig. 5. It is obvious that the pressure drop is higher for lower aspect ratios. Pressure drop in micro/nano-channels decreases with increase in aspect ratios.

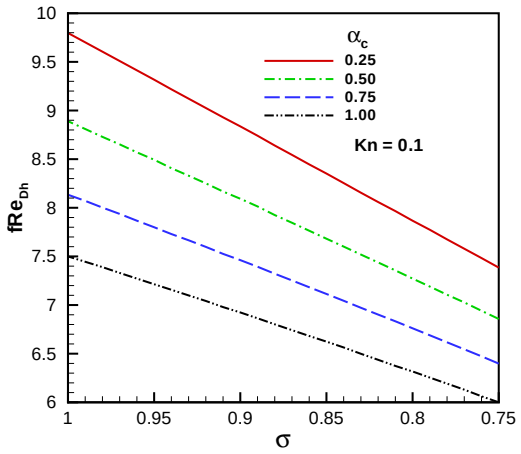

Fig. 4 EFFECT OF TMAC ON FRICTION FACTORS

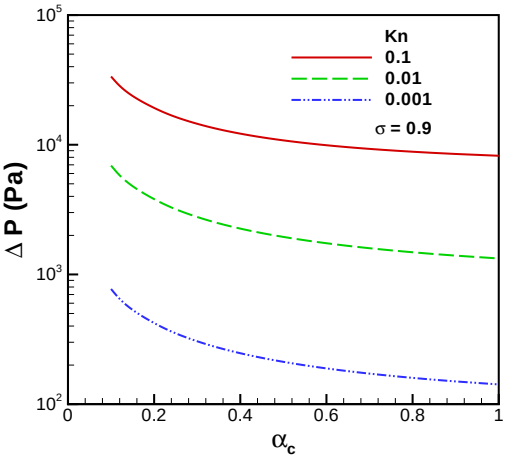

Fig. 5 EFFECT OF Kn ON PRESSURE DROP

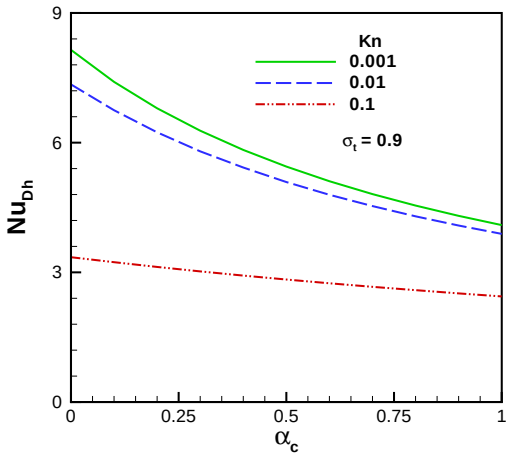

Fig. 6 EFFECT OF α_c ON HEAT TRANSFER FROM FIN IN SLIP FLOW REGION

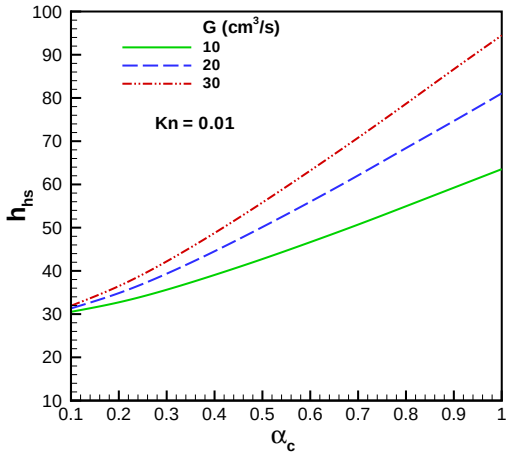

Fig. 7 EFFECT OF VOLUME FLOW RATE ON AVERAGE HEAT TRANSFER FROM MICRO/NANO-CHANNEL HEAT SINK

The dimensionless heat transfer coefficient decreases with increase in Knudsen numbers and aspect ratios as well. This trend is shown in Fig. 6. The effect of Kn number is to decrease the value of the Nusselt number below its continuum value, and the reduction increases significantly with increasing Kn number. Figure 7 shows the effect of volume flow rate on the average heat transfer from a micro/nano-channel heat sink. It is obvious that the average heat transfer increases with the increase in volume flow rate and aspect ratio.

CONCLUSIONS

Continuum momentum and energy equations are solved for laminar forced convection in two-dimensional rectangular micro and nano-channels under hydrodynamically and thermally fully developed conditions with the first-order velocity slip and temperature jump boundary conditions at the channel walls. Closed form solutions are obtained for fluid friction and Nusselt numbers in the slip flow regime $(0.001 < Kn < 0.1)$. It is demonstrated that:

1. The channel width ranges from 350 *nm* to 35μm.
2. The friction losses decrease with the decreasing in Knudsen number and increasing in channel aspect ratio.
3. The friction factors decrease with the decrease in tangential momentum accomodation coefficients.
4. The pressure drop in the channels decreases with the increase in aspect ratios.
5. The dimensionless heat transfer coefficient for the channel decreases with the increase in Knudsen numbers and aspect ratios as well.
6. The average heat transfer coefficient of the heat sink increases with the increase in volume flow rate and aspect ratios.

ACKNOWLEDGMENTS

The authors gratefully acknowledge the financial support of Natural Sciences and Engineering Research Council of Canada and the Center for Microelectronics Assembly and Packaging.

REFERENCES

1. Tuckerman, D. B., and Pease, R. F. W., High-Performance Heat Sinking for VLSI, IEEE Electron Device Letter, EDL-2, pp. 126-129, 1981.
2. Harley, J.C., Huang, Y., Bau, H.H., Zewel, J.N., "Gas flow in micro-channels," Journal of Fluid Mech. Vol. 284, pp. 257-274, 1995.
3. Morini, G.L. , Spiga, M., "Slip Flow in Rectangular Microtubes," Microscale Thermophysical Engineering, Vol. 2, No. 4, pp. 273-282, 1998.
4. Morini, G.L., Spiga, M., Tartarini, P., "The Rarefaction Effect on the Friction Factor of Gas Flow in Micro/Nano-Channels," Superlattices and Microstructures, Vol. 35, No. 3-6, pp. 587-599, 2004.
5. Morini, G. L., Lorenzini, M., and Spiga, M., "A Criterion for Experimental Validation of Slip-Flow Models for Incompressible Rarefied Gases Through Micro/Nano-Channels," Microfluidics and Nanofluidics, Vol. 1, No. 2, pp. 190-196, 2005.
6. Ebert, W.A. and Sparrow, E.M., "Slip Flow in Rectangular and Annular Ducts," Trans. ASME, J. Basic Engineering, Vol. 87, pp. 1018-1024, 1965.
7. Inman, R. M., "Heat Transfer For Laminar Slip Flow of a Rarefied gas in a Parallel Plate Channel or a Round Tube

With Uniform Wall Heating," NASA TN D-2393, August, 1964.
8. Inman, R. M., "Heat Transfer For Laminar Slip Flow of a Rarefied gas in a Parallel Plate Channel or a Circular Tube With Uniform Wall Temperature," NASA TN D-2213, November, 1964.
9. Inman, R. M., "Heat Transfer For Laminar Slip Flow of a Rarefied gas Between Parallel Plates With Unsymmetrical Wall Heat Flux," NASA TN D-2421, August, 1964.
10. Colin, S., Lalonde, P., and Caen, R., "Validation of a Second-Order Slip Flow Model in Rectangular Micro/Nano-Channels," Heat Transfer Engineering, Vol. 25, No. 3, pp. 23-30, 2004.
11. Yu, S. and Ameel, T. A., "Slip Flow Heat Transfer in Rectangular Micro/Nano-Channels," International Journal of Heat and Mass Transfer, Vol. 44, pp. 4225-4234, 2001.
12. Yu, S. and Ameel, T. A., "Slip Flow Convection in Isoflux Rectangular Micro/Nano-Channels," Journal of Heat Transfer, Vol. 124, pp. 346-355, 2002.
13. Zhao, C.Y., Lu, T.J. "Analysis of Micro/Nano-Channel Heat Sinks for Electronics Cooling," International Journal of Heat and Mass Transfer, Vol. 45, pp. 4857-4869, 2002.
14. Quarmby, A., "A Finite-Difference Analysis of Developing Slip Flow," Applied Scientific Research, Vol. 19, pp. 18-33, 1968.
15. Gampert, B., "Inlet Flow With Slip. Rarefied Gas Dynamics," Vol. 10, pp. 225-235, 1976.
16. Barber, R.W. and Emerson, D.R., "A Numerical Investigation of Low Reynolds Number Gaseous Slip Flow at the Entrance of Circular and Parallel Plate Micro/Nano-Channels," ECCOMAS Computational Fluid Dynamics Conference 2001 Swansea, Wales, UK, 4-7 September 2001.
17. Barber, R.W. and Emerson, D.R., "The Influence of Knudsen Number on the Hydrodynamic Development Length Within Parallel Plate Micro-channels," Advances in Fluid Mechanics IV Eds. Rahman, M., Verhoeven, R. and Brebbia, C.A., WIT Press, Southampton, UK, pp. 207-216, 2002.
18. Andrei G. F., and Raymond V., "Three-Dimensional Conjugate Heat Transfer in the Micro/Nano-Channel Heat Sink for Electronic Packaging," International Journal of Heat and Mass Transfer, Vol. 43, No. 3, pp. 399-415, 2000.
19. Arkilici, E. B., Breuer, K. S. and Schmidt, M. A., "Mass Flow and Tangential Momentum Accommodation in Silicon Micromachined Channels," Journal of Fluid Mechanics, Vol. 437, pp. 29-43, 2001.
20. Arkilici, E. B., Schmidt, M. A., and Breuer, K. S., "Gaseous Slip Flow in Long Micro/Nano-Channels, Journal of Microelectromechanical Systems," Vol. 6, No. 2, pp. 167-178, 1997.
21. Beskok, A. and Karniadakis, G. E., "A Model for Flows in Channels, Pipes, and ducts at Micro Scales," Microscale Thermophysical Engineering, Vol. 3, pp. 43-77, 1999.
22. Bower, C., Ortega, A., Skandakumaran, P., Vaidyanathan, R., Green, C., Phillips, T., "Heat Transfer in Water-Cooled Silicon Carbide Milli-Channel Heat Sinks for High Power Electronic Applications," 2003 ASME International Mechanical Engineering Congress & Exposition Washington, D.C., November 16-21, 2003.
23. Harms, T. M., Kazmierczak, M. J., Gerner F. M., "Developing Convective Heat Transfer in Deep Rectangular Micro/Nano-Channels," International Journal of Heat and Fluid Flow, Vol. 20, pp. 149-157, 1999.
24. Hetsroni, G., Mosyak, A., Pogrebnyak, E., and Yarin, L.P., "Fluid Flow in Micro-Channels," International Journal of Heat and Mass Transfer, Vol. 48, pp. 1982-1998, 2005.
25. Hetsroni, G., Mosyak, A., Pogrebnyak, E., and Yarin, L.P., "Heat Transfer in Micro-Channels: Comparison of Experiments with Theory and Numerical Results," International Journal of Heat and Mass Transfer, Vol. 48, pp. 5580-5601, 2005.
26. Hsieh, S.S., Tsai, H.H., Lin, C.Y., Huang, C.F., and Chien, C. M., "Gas Flow in Long Micro/Nano-Channel, International Journal of Heat and Mass Transfer, Vol. 47, pp. 3877-3887, 2004.
27. Hsieh, S. S., Lin, C. Y., Huang, C. F. and Tsai, H. H., "Liquid Flow in a Micro/Nano-Channel," Journal of Micromechanics and Microengineering, Vol. 14, pp. 436-445, 2004.
28. Eckert, E. R. G. and Drake, R. M., "Analysis of Heat and Mass Transfer," Chap. 11, McGraw-Hill, New York, 1972.
29. Liu, D., and Garimella, S. V.,"Analysis and Optimization of the Thermal Performance of Micro/Nano-Channel Heat Sinks", International Journal for Numerical Methods in Heat & Fluid Flow, Vol. 15, No. 1, pp. 7-26, 2005.
30. Shah, R.K., London, A.L., "Laminar Flow Forced Convection in Ducts," Advances in Heat Transfer, Vol. 14, suppl. I, 1978. 196.
31. Kleiner, M.B., Kuhn, S.A., and Haberger, K., "High Performance Forced Air Cooling Scheme Employing Micro/Nano-Channel Heat Exchangers," IEEE Transactions on Components, Packaging, and Manufacturing Technology, Part A, Vol. 18, Issue 4, pp. 795 - 804, 1995.
32. Kays, W. M. and London, A. L., "Compact Heat Exchangers," McGraw Hill, New York, 1964.
33. Khan, W. A., Culham, J. R., and Yovanovich, M. M., "Fluid Flow Around and Heat Transfer from Elliptical Cylinders: Analytical Approach," Journal of Thermophysics and Heat Transfer, Vol. 19, No. 2, 2005.
34. Qin, J. S. J. and Li, W. J., "Fabrication of Complex Micro Channel Systems Inside Optically-Transparent 3D Substrates by Laser Processing," 11th International Conference on Solid-State Sensors and Actuators, Munich, Germany, June 2001.